Determination of the Resolution for Relative Beam Energy Measurement of the 4-Magnet Chicane in the Experiment T474/491

Michele Viti*

Deutsches Elektronen-Synchrotron DESY

15738 Zeuthen, Germany

June 15, 2009

Abstract

*michele.viti@desy.de

1 General Considerations

During 2007 a complete 4-magnet chicane was implemented in ESA so that beam energy measurements could be performed[1, 2]. Here only some general arguments are summarized needed for evaluation of the resolution for relative beam energy measurements. The structure of this chapter as follows. In Sect. 2 an overview of the 4-magnet chicane is given. In Sect. 3 the BPMs within the A-line (energy BPMs) will be discussed and their resolution determined. Sect. 4 evaluates the resolution of the 4-magnet chicane and compares the results from the energy BPMs. The last section contains the conclusions.

The data were collected in "runs", where one run was typically 10-20 minutes of data taking time. The data were stored by a Labview program running on a Windows XP computer and, after some reorganization, saved in root files.

During a given run the field of the magnets was fixed and only changed periodically for positive polarity, zero current and negative polarity runs. Several operation modes such as energy scans and calibration procedures were performed. Calibration runs were carried out using the corrector dipoles, Helmholtz coils and mover systems.

Energy scans were performed by changing the beam energy from the nominal value E_{beam}^{nom} of 28.5 GeV in 5 steps of 50 MeV between $E_{beam}^{nom} \pm 0.1$ GeV (200 MeV total range). In the following only these data will be accounted for.

2 The 4-Magnet Chicane in End Station A

In Fig. 1 a schematic view of the 4-magnet chicane in ESA is shown. The magnets were installed on a girder, using supports made of non-ferromagnetic material. Only one power supply was used with the magnets mounted in series, so that the current was the same for all of them. Through a display of a Linux computer it was possible to set the nominal values of the B-field integral for the magnets. The nominal values are converted in a current value by the control program, using a linear relation[3]. In Fig. 1 the main instruments are also visible. The magnet 3B1 was equipped with two NMR probes and one Hall probe, whereas the other magnets have only one NMR probe. The current value used was $\pm$ 150 A, which corresponds roughly to a B-field of $\pm$ 1.1 kG in order to achieve 5 mm offset in the mid-chicane for an electron beam of 28.5 GeV. The two NMR probes in 3B1 are different types, so that different working ranges are covered. They overlap in the region of

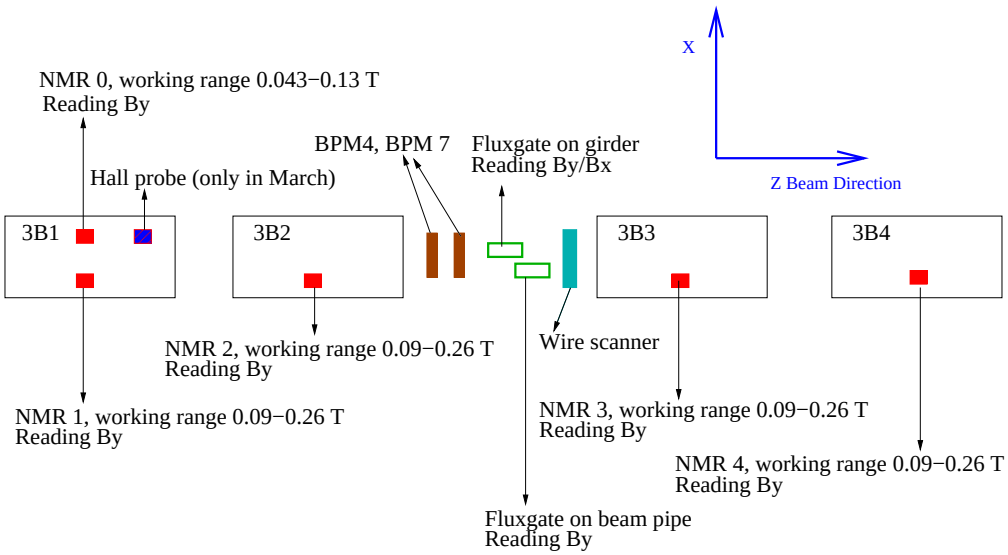

Figure 1: Schematic representation of the four-magnet chicane in ESA. The main instruments are shown

the B-field settings. The Hall probe was placed in magnet 3B1 only for the run in March 2007, removed after that to be used in the wiggler magnet for experiment T475.

Along the beam line, two flux gate monitors were placed to have access to the stray fields: one was placed on the girder to read the X- and Y-components of the stray fields and the other on the beam pipe reading only the Y-component.

3 Energy BPMs

Along the bend in the A-line some BPMs are placed which provide through the X-position readings a measurement of the relative variation of E_b, the nominal beam energy. The data available in the files are the X-position and the tilt in the XZ-plane from BPMs 12 and 24. These variables are denoted as x24Pos, x12Pos, x24Tilt and x12Tilt in the following. At these locations in the A-line the X-positions and the tilts θ of the beam are coupled with the energy through $E \propto 1/x \propto 1/\theta$, where any position jitter of the beam is neglected. Thus, for the relative energy resolution we have

$$\frac{\sigma_{E_b}}{E_b} = \frac{\sigma_{\mathrm{X}}}{\mathrm{x}} \ , \tag{1}$$

where x represents one of the variables x24Pos, x12Pos, x24Tilt and x12Tilt.

In a first step, all the quantities to be used must be normalized in order to be able to compare them. Denoting with x a generic raw variable, the normalized quantity x' is defined as

$$x' = \frac{x - \bar{x}}{\Delta_x} \ , \tag{2}$$

where $\bar{x}$ is the mean value and Δ_x the standard deviation of x calculated for a given number of events. The data shown in Figs. 2 and 3 (each point corresponds to a particular bunch) are from an energy scan performed during a run where the current of the magnets was set at +150 A. The five energy steps of the scan at E_b-100 MeV, E_b-50 MeV, E_b, E_b+50 MeV, E_b+100 MeV are clearly visible. Fig. 2 explains the normalization procedure with an example: the raw X-position data of BPM 12 are shown for some events where an energy scan was performed (left). Since the BPM is not calibrated the Y-scale is given in arbitrary units. The histogram on the right-hand side is the projection of the data in Fig. 2 (left) to the Y-axis. Thus, the mean value $\bar{x}$ and the RMS Δ_x can be calculated. It is important to note that Δ_x and the σ's in Eq.(1) are different quantities. The first quantity represents the width of the scan data used for normalization while the latter ones are the errors on position and tilt measurements.

An example of the result of a data normalization is given in Fig. 3, where the raw X-position readings of BPM 12 and 24 (left) and the normalized data (right) are shown for an energy scan. The raw x24Pos measurements have a different mean value and standard deviation compared to BPM 12 data but, after normalization, x12Pos and x24Pos data superimpose perfectly. In the following plots the normalized Y-scale will be always referred as "a.u.", arbitrary units. As can be also seen, for a fixed beam energy the response of the BPMs is a cluster of points which is mainly due to the beam energy jitter.

The two dashed lines, visible in the right-hand side of Fig. 3, indicate the total range in energy where the scan was performed. This range is about 3 for the normalized scale while corresponds to 200 MeV in terms of beam energy. This correspondence provides the scale factor.

3.1 Energy BPM Resolution

Considering the normalized variables x24Pos, x12Pos, x24Tilt, x12Tilt as independent, it is possible to calculate their resolutions, by means of the histograms in Fig. 4. Each histogram represents, for a particular energy

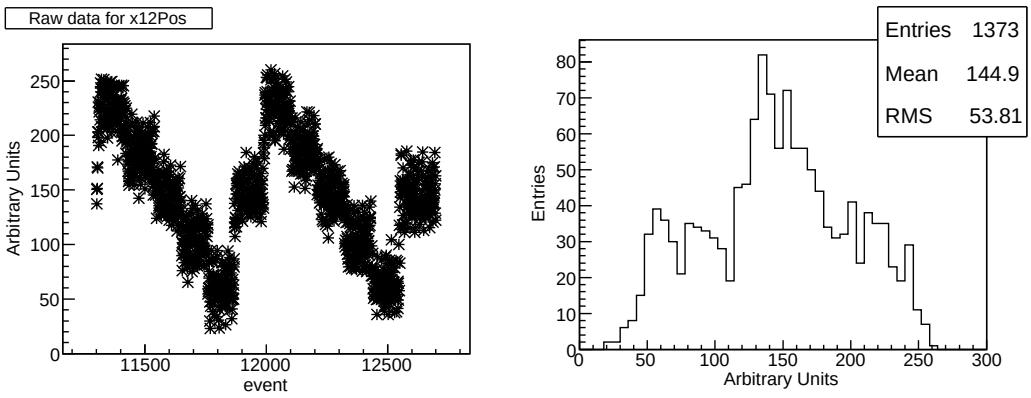

Figure 2: Raw X-position readings for BPM 12 for an energy scan (left). The data plotted in a histogram allow to calculate their mean value and RMS for normalization purpose(right).

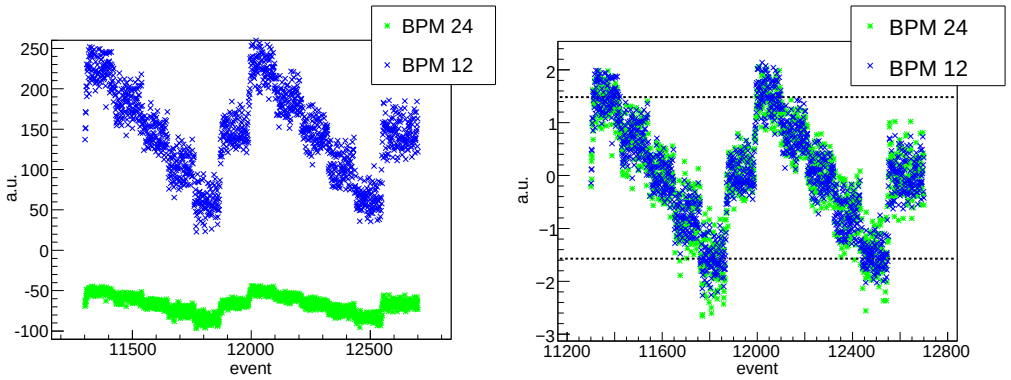

Figure 3: Raw (left) and normalized (right) variables x12Pos and x24Pos for an energy scan. The two dashed lines on the right-hand side indicate the scan range used.

scan, the difference between two of the four variables, event by event. Not all possible combinations are shown. It is important to note that the difference between two quantities with different dimensions, like position and tilt, is now physically meaningful since they are normalized.

From Fig. 4 we obtain

$$\begin{cases} \sigma_1^2 &=& \sigma_{x24Pos}^2 + \sigma_{x12Pos}^2 &=& (0.1865)^2 \\ \sigma_2^2 &=& \sigma_{x24Pos}^2 + \sigma_{x12Tilt}^2 &=& (0.2151)^2 \\ \sigma_3^2 &=& \sigma_{x12Pos}^2 + \sigma_{x24Tilt}^2 &=& (0.1231)^2 \\ \sigma_4^2 &=& \sigma_{x12Pos}^2 + \sigma_{x12Tilt}^2 &=& (0.125)^2 \ . \end{cases} \tag{3}$$

Considering the measurements as independent and neglecting possible position jitters, all σ's should be zero for an ideal situation. Any non-zero value indicates a finite resolution of the device. Solving the system(3) for σ_{x24Pos}, σ_{x12Pos}, $\sigma_{x24Tilt}$ and $\sigma_{x12Tilt}$ we obtain

$$\begin{cases} \sigma^{a.u.}_{x24Pos} &= 0.187 \\ \sigma^{a.u.}_{x12Pos} &= 0.018 \\ \sigma^{a.u.}_{x24Tilt} &= 0.12 \\ \sigma^{a.u.}_{x12Tilt} &= 0.124 \ , \end{cases} \tag{4}$$

where $\sigma^{a.u.}$ means that the quantity is expressed in arbitrary units of the normalized scale. According to Eqs.(1) and (2), we have

$$\frac{\sigma^{a.u.}}{3} = \frac{\sigma^{MeV}}{200} \ , \tag{5}$$

so σ^{MeV}_{x12Pos}, defined as the resolution of the variable x12Pos for a relative beam energy measurement, can be written as $\sigma^{MeV}_{x12Pos} = 0.018 \cdot 200/3 = 1.2$ MeV, which corresponds to

$$\frac{\sigma^{MeV}_{x12Pos}}{E_b} = \frac{1.2 \text{ MeV}}{28.5 \text{ GeV}} = 4.2 \times 10^{-5} \ . \tag{6}$$

It is important to remark that the energy BPMs do not provide an absolute but only a relative beam energy measurement, i.e. no determination of E_b is possible.

4 ESA Magnet Chicane

In 2007 March runs the readout of the probes was not working properly and in July runs the two NMR probes installed in magnet 3B1 and the one installed in 3B3 were damaged. Thus, fundamental informations for absolute beam energy measurements were missing. Moreover, an independent method for an absolute beam energy measurement E_b was a priori not foreseen in ESA so that the results from the magnet chicane can not be cross-calibrated. Hence, only relative beam energy measurements can be performed with the BPM-spectrometer.

4.1 Mid-chicane BPM 4

For the following analysis, only the data from runs in July 2007 will be used. Since BPM 7, also positioned in the mid-chicane, was considered to be not

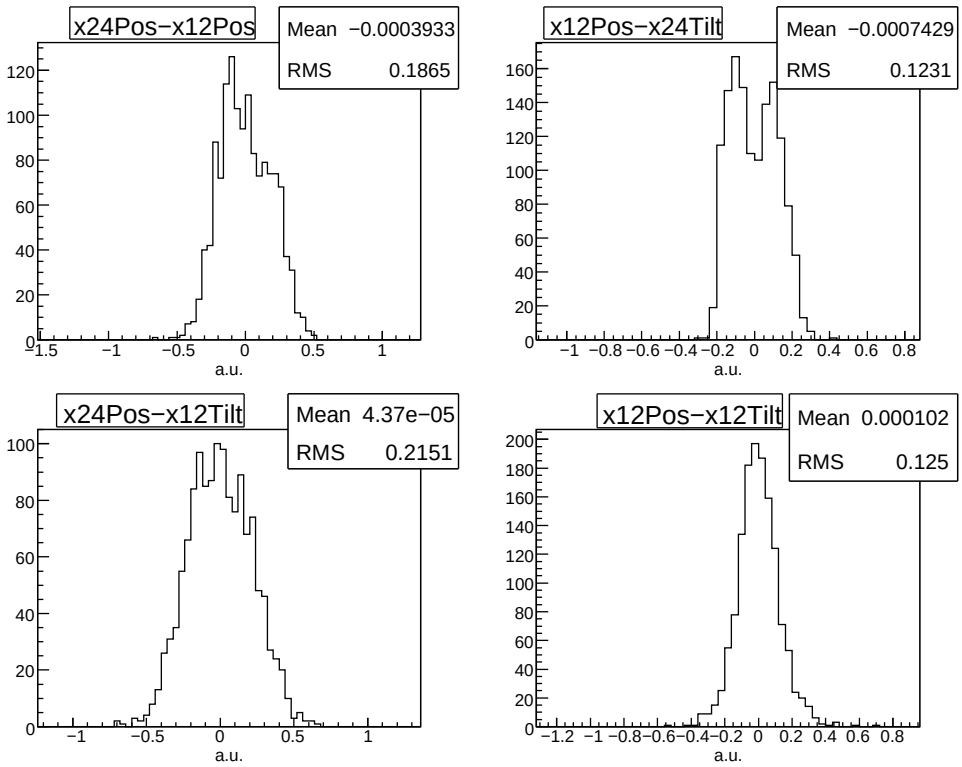

Figure 4: Differences between the variables as indicated for an energy scan.

reliable, only data from BPM 4 will be employed. If not explicitly stated, all variables considered are not normalized.

Selecting the energy scan data from run 2743, Fig. 5 shows the X-readings of BPM 4 (x4Pos). In this case, any steps in energy cannot be recognized as in Fig. 3 since position fluctuations of the beam are bigger than the energy steps applied.

In fact, referring to Fig. 6, the quantity $x^{(4)}_{chicane}(E_b)$ can be written as

$$x^{(4)}_{chicane}(E_b) = \text{x4Pos} + A - x^{(4)}_{jitter} \ , \tag{7}$$

where $x^{(4)}_{chicane}(E_b)$ is the beam offset in the mid-chicane at the Z-position of BPM 4, which is coupled with energy through $E \propto 1/x$, $x^{(4)}_{jitter}$ the extrapolation of beam in the mid-chicane at the same Z-position and A a BPM offset, which ensures to position the beam close to the center of the BPM. The value of A can vary if the B-field is modified (for example when switching the magnet polarity or when running with zero-magnet current). Nevertheless, since we normalize our data, this offset is not important at all and allows us to

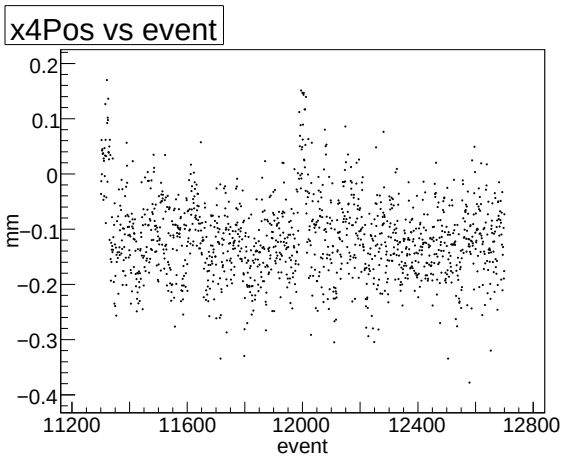

Figure 5: Beam position values of BPM 4 (without normalization) of an energy scan. The size of possible beam position jitters covers completely possible variations of the energy itself.

write:

$$\text{x4Pos} = x^{(4)}_{chicane}(E_b) + x^{(4)}_{jitter} \ . \tag{8}$$

In order to have access to the offset $x^{(4)}_{chicane}(E_b)$ it is necessary to subtract the quantity $x^{(4)}_{jitter}$ obtained from extrapolation of the beam positions from BPMs 1,2,3,5,9,10,11, from x4Pos. It is obvious that for zero-current, $x^{(4)}_{chicane}(E_b) = 0$ and, hence, x4Pos=$x^{(4)}_{jitter}$

4.2 Evaluation of $x^{(4)}_{jitter}$

The simplest way to determine $x^{(4)}_{jitter}$ is performing a simple linear fit through the BPMs upstream and downstream of the chicane and extrapolating the straight line to the Z-position of BPM 4. This method is, however, limited by a) not taking into account any coupling between X- and Y-positions of the BPMs, b) other informations as the tilt are usually not accounted for, since rotation or misalignment of the BPMs are difficult to implement into the analysis and c) the offset between centers of the BPMs should be known accurately, whose determination is also a non-trivial task.

Fig. 7 shows the $x^{(4)}_{jitter}$ values calculated from BPMs 1,2,3,5 upstream of the chicane. The data are from a run, where the magnet current was set to zero, hence, x4Pos = $x^{(4)}_{jitter}$. The dashed line in Fig. 7 represents a straight line with a slope of 1. It is evident that x4Pos = $\alpha \cdot x^{(4)}_{jitter}$, with $\alpha \neq 1$,

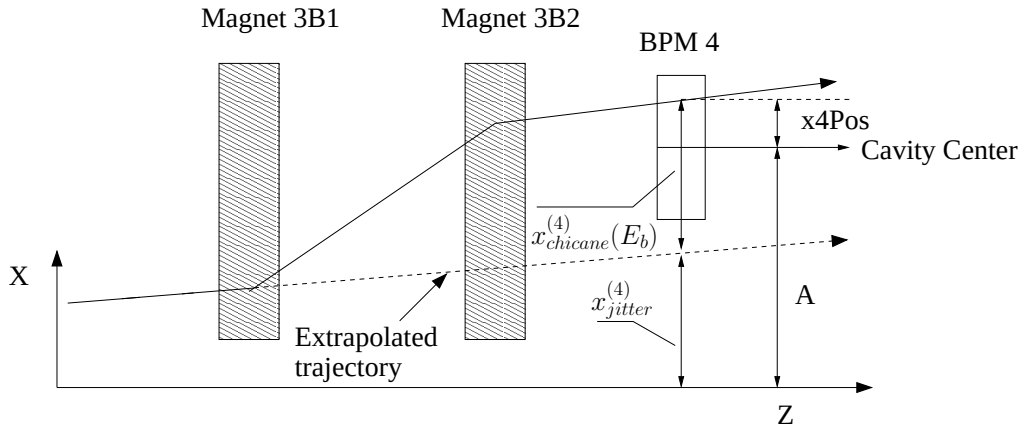

Figure 6: Schematic representation of the working principle of a magnet chicane: a charged particle traveling through the spectrometer receives an additional offset inversely proportional to its energy. The X-position reading of BPM 4 is thus the sum of two quantities, namely the extrapolated position $x^{(4)}_{jitter}$ and the offset $x^{(4)}_{chicane}(E_b)$.

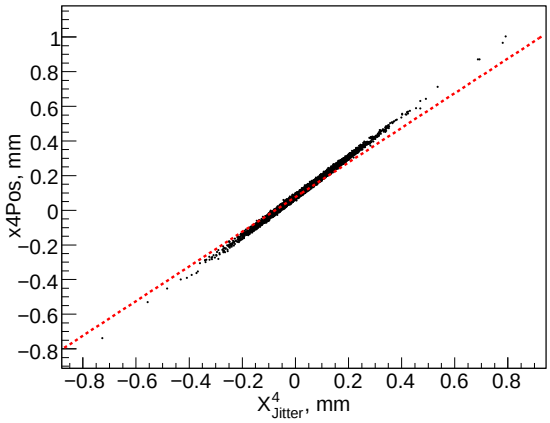

Figure 7: BPM 4 position measurement vs $x^{(4)}_{jitter}$ evaluated from a linear extrapolation using the X-positions from BPMs 1,2,3,5.

which might be due to different rotations of the BPMs around the Z-axis. In general, x4Pos can be written as

$$\text{x4Pos} = \alpha \cdot x^{(4)}_{jitter} + \beta \cdot x^{(4)}_{chicane}(E_b) \ , \tag{9}$$

where β represents a possible relative rotation of the BPM with respect to dipole field.

Thus, a more appropriate approach is necessary to predict the correct value of $x^{(4)}_{jitter}$, with $\alpha = 1$ in (9) (a discussion on β will be presented later, but for the moment it is set to 1). One possibility for $x^{(4)}_{jitter}$ evaluation relies on the assumption that this variable depends linearly on other BPM variables positioned upstream and/or downstream of the chicane. Fig. 8 shows an example: x4Pos is plotted against x5Pos and x5Tilt from BPM 5. The variables are not normalized and are taken from a run with zero-current (run 2747). A clear correlation is present in both cases.

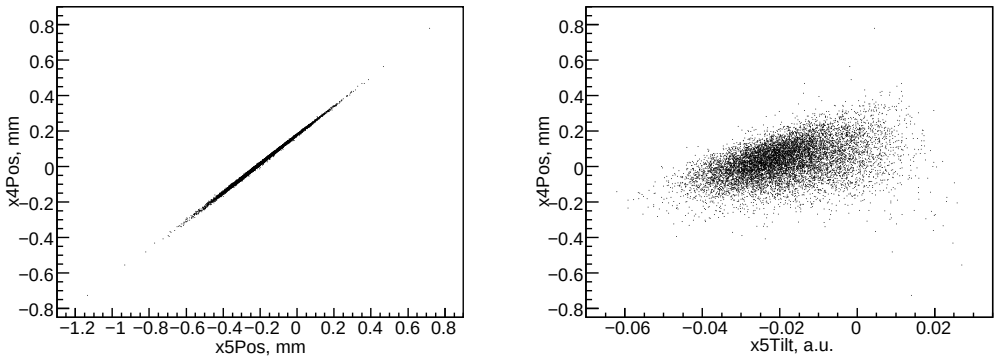

Figure 8: x4Pos as a function of x5Pos (left) and x5Tilt (right) for a run with zero-current.

Under this assumption the beam jitter at BPM 4 can be written as

$$\begin{aligned} x^{(4)}_{jitter} \;=\; & c^0 + c^1_1 \cdot \mathrm{x1Pos} + c^2_1 \cdot \mathrm{x1Tilt} + c^3_1 \cdot \mathrm{y1Pos} + c^4_1 \cdot \mathrm{y1Tilt} \\ & \vdots \\ & + c^1_j \cdot \mathrm{xjPos} + c^2_j \cdot \mathrm{xjTilt} + c^3_j \cdot \mathrm{yjPos} + c^4_j \cdot \mathrm{yjTilt} \\ & \vdots \\ & + c^1_N \cdot \mathrm{xNPos} + c^2_N \cdot \mathrm{xNTilt} + c^3_N \cdot \mathrm{yNPos} + c^4_N \cdot \mathrm{yNTilt}\ , \end{aligned} \tag{10}$$

where xjPos and yjPos denote the X-, respectively, Y-position, xjTilt and yjTilt the corresponding tilts of the j-th BPM and N the total number of BPMs used. For a run with magnet current set to zero, the coefficients c^j_i are determined minimizing the quantity

$$\sum_{i=1}^{N_{event}} (\mathrm{x4Pos} - x^{(4)}_{jitter})^2_i\ . \tag{11}$$

The results are discussed in Sect. 4.4.

4.3 Dipole Magnets

The fundamental prerequisite of the spectrometer is that the beam position downstream of the chicane is not coupled with that within the chicane, which means that the upstream beam path must be restored downstream, i.e. the chicane has to act in a symmetric manner. Measurements performed in March 2007 to study the response of the chicane consisted, for a given nominal B-field, in measuring the B-field of the magnets. The results are given in Fig. 9. Here, the difference between the measured and the nominal B-field is plotted as a function of the nominal value, for negative and positive currents.

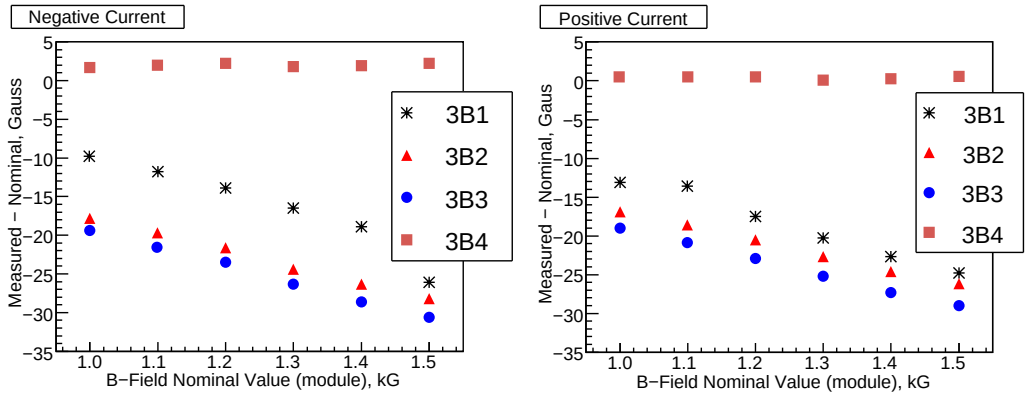

Figure 9: Differences between the measured and nominal B-fields as a function of the nominal value of the four magnets in ESA. Left: negative current. Right: positive current.

For magnet 3B1 the measurement was performed using only the Hall probe, whereas for the other magnets NMR probes were used. As can be seen, the differences vary from few Gauss (for magnets 3B2 and 3B3) up to $\sim$ 30 Gauss. Magnet 3B4 shows field values closer to the nominal ones, because the relation discussed in Sect. 4 and used to calculate the magnet current, was determined in the laboratory for this magnet. The differences seen in the figure might be due to any residual field, which was estimated to be 2-4 Gauss and depends on the history of the magnet, and differences on steel magnetic properties as no careful design and composition of the steel was accounted for. As a consequence, downstream of the chicane the upstream path of the beam is not fully restored and changes of the beam energy are converted to position variations in BPMs 9, 10 and 11. Similarly

to what was done for BPM 4, the X-position of BPM 9 can be written as

$$\text{x9Pos} = x^{(9)}_{jitter} + x^{(9)}_{chicane}(E_b) \ , \tag{12}$$

For simplicity, the factors α and β are set equal to 1. If, in analysis, BPM 1, 2, 3 and 5 are used to predict the X-position at BPM 9 ($x^{(9)}_{jitter}$) and this value is then subtracted from x9Pos for an energy scan, $x^{(9)}_{chicane}(E_b)$, as shown in Fig 10, is obtained. Although no perfectly, the steps due to different beam energies are clearly visible, demonstrating that for BPM 9, $x^{(9)}_{chicane}(E_b)$ is different from zero.

This observation also clearly reveals that the BPMs downstream of the chicane cannot be used to estimate the beam jitter in BPM 4, $x^{(4)}_{jitter}$.

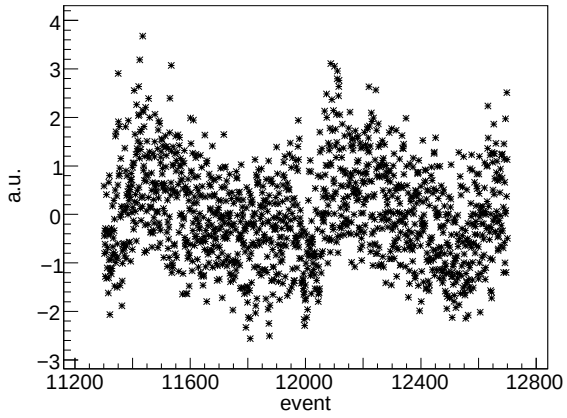

Figure 10: Normalized beam position of BPM 9 for an energy scan after subtraction of the prediction from BPMs 1, 2, 3 and 5. The energy variation is clearly visible.

4.4 4-Magnet Chicane Resolution

Using data from zero-current run, the parameters c^j_i were determined minimizing the quantity(11) as described in Sect. 4.2, by accounting for X-, Y-position and the X-, Y-tilt data from BPMs 1, 2, 3 and 5.[1]

Using the resulting coefficients c^j_i in Eq.(10), $x^{(4)}_{jitter}$ can be calculated and if x4Pos is now plotted against the new $x^{(4)}_{jitter}$ for a zero-current run, a

[1]If only only X-position and X-tilt are taken into account less precise results are obtained, see discussions later.

straight line behavior, with a slope close to 1, can be recognized, see Fig. 11. This finding demonstrates that the evaluation of $x^{(4)}_{jitter}$ using Eq.(10) is much more appropriate than the procedure given at the beginning of Sect. 4.2.

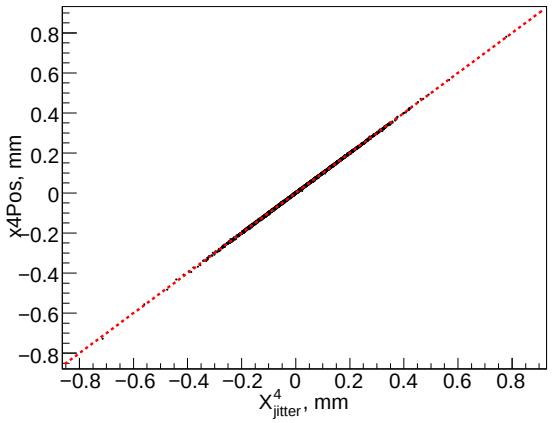

Figure 11: The position x4Pos versus $x^{(4)}_{jitter}$ evaluated using Eqn. 10. The data are from a run with magnet current set to zero.

4.4.1 Beam Energy Resolution

The evaluation of relative beam energy resolution of the 4-magnet chicane was performed in the following way. Considering an energy scan with magnet current of +150 A, after subtraction of $x^{(4)}_{jitter}$ from x4Pos the beam offset in the mid-chicane $x^{(4)}_{chicane}(E_b)$ is obtained (see Eq.(8)).

$x^{(4)}_{chicane}(E_b)$ is then normalized and subtracted to the corresponding normalized X-position BPM 12 measurements. In Fig. 12 (left) the normalized x12Pos and $x^{(4)}_{chicane}(E_b)$ variables are superimposed, while on the right-hand side the difference (x12Pos - $x^{(4)}_{chicane}(E_b)$) is presented. The non-zero value of the standard deviation given in arbitrary units, $\sigma^{a.u.}$, of the histogram is due to a finite resolution of $x^{(4)}_{chicane}(E_b)$ and x12Pos. In fact

$$\sigma^{a.u.} = \sigma^{a.u.}_{x^{(4)}_{chicane}(E_b)} \oplus \sigma^{a.u.}_{x12Pos} = 0.365 \ , \tag{13}$$

where the terms are added in quadrature. $\sigma^{a.u.}_{x12Pos}$ was evaluated to be 0.0187 in Sect. 3.1 and, hence, negligible so that

$$\sigma^{a.u.} \simeq \sigma^{a.u.}_{x^{(4)}_{chicane}(E_b)} \simeq 0.365 \ . \tag{14}$$

$\sigma^{a.u.}_{x^{(4)}_{chicane}(E_b)}$ can be understood as the beam energy resolution of the 4-magnet chicane. From Eq.(5), we have

$$\sigma^{MeV}_{x^{(4)}_{chicane}(E_b)} = \sigma_{E_b} = 0.365 \cdot 200/3 = 24.3 \text{ MeV}$$
$$\rightarrow \frac{\sigma_{E_b}}{E_b} = \frac{24.3 \text{ MeV}}{28.5 \text{ GeV}} = 8.5 \times 10^{-4} \ . \tag{15}$$

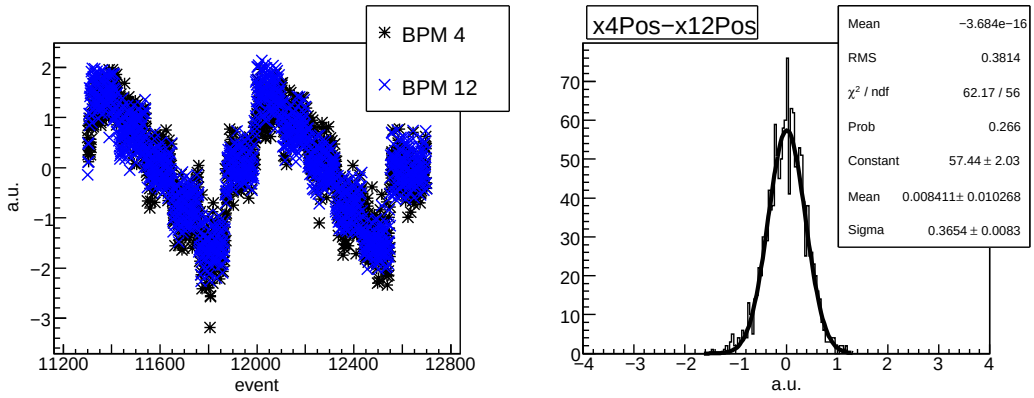

Figure 12: Left: Normalized position x4Pos after subtraction of the jitter ($x^{(4)}_{chicane}(E_b)$) and the position x12Pos, for an energy scan with the magnet current of +150 A. Right: Difference between $x^{(4)}_{chicane}(E_b)$ and x12Pos.

If only the X-positions and X-tilts from BPMs 1, 2, 3 and 5 are taken into account, $x^{(4)}_{jitter}$ is less precise and the energy resolution results to $\sigma_{E_b}/E_b \simeq 8.9 \times 10^{-4}$. This value is, however, close to that in Eq.(15), which reveals that the variables yPos and yTilt have no strong impact on $x^{(4)}_{jitter}$.

In principle, the relative energy resolution can be, estimated in a complementary way. Since $x^{(4)}_{chicane}(E_b) =$ x4Pos - $x^{(4)}_{jitter}$, the resolution of $x^{(4)}_{chicane}(E_b)$ is equivalent to the resolution of (x4Pos - $x^{(4)}_{jitter}$).

Fig. 13 shows (x4Pos - $x^{(4)}_{jitter}$) for a run with zero-current. Hence, (x4Pos - $x^{(4)}_{jitter}$) is expected to be zero for every event, but the standard deviation is non-zero. Interpreting this quantity as the resolution of (x4Pos - $x^{(4)}_{jitter}$), respectively, $x^{(4)}_{chicane}(E_b)$ and accounting for $x^{(4)}_{chicane}(E_b) \approx 5$ mm in the mid-chicane (see Sect. 2), Eq. 1 becomes

$$\frac{\sigma_{x^{(4)}_{chicane}(E_b)}}{x^{(4)}_{chicane}(E_b)} = \frac{\sigma_{E_b}}{E_b} = \frac{2.3 \ \mu\text{m}}{5 \text{ mm}} = 4.6 \times 10^{-4} \ . \tag{16}$$

This result is considerably better than that of (15). Possible reasons for the difference might be the non-demagnetization after switching off the magnets and/or the factor β in Eq.(9). In fact, if there is some rotation of the BPM 4 with respect to the dipole field by an angle θ, the effective offset at the mid-chicane is 5 mm $\cdot \cos\theta$ and the error on relative beam energy measurements becomes

$$\frac{\sigma_{E_b}}{E_b} = \frac{2.3\ \mu\text{m}}{5\ \text{mm} \cdot \cos\theta} > 4.6 \times 10^{-4}\ . \tag{17}$$

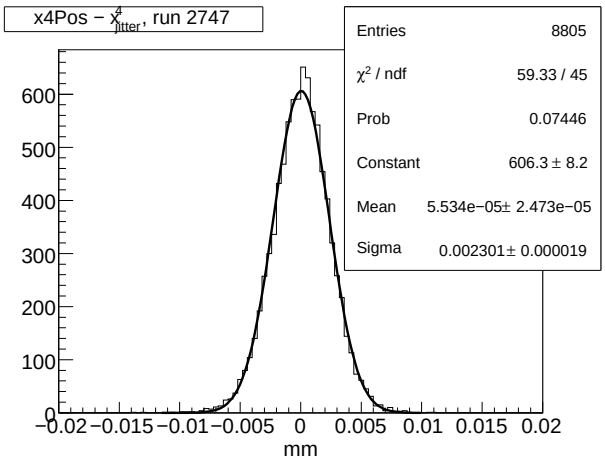

Figure 13: Difference between x4Pos and $x^{(4)}_{jitter}$ for a zero-magnet current. $x^{(4)}_{jitter}$ is calculated using the parameters extracted from a minimization procedure as described in Sect.4.2

4.5 X- and Y-Position Coupling

In analogy to the X-position determination it is possible to estimate $y^{(4)}_{jitter}$ and, after subtraction from y4Pos, $y^{(4)}_{chicane}(E_b)$ is obtained. In Fig. 14, $y^{(4)}_{chicane}(E_b)$ is plotted against $x^{(4)}_{chicane}(E_b)$ for an energy scan. Some coupling is clearly visible, which reveals that the parameter β in Eq.(9) is definitely different from 1. This can be due to the fact that BPM 4 is rotated around the Z-axis with respect to the magnetic field as already stated in the previous section. Thus, to improve the relative beam energy resolution, also the $y^{(4)}_{chicane}(E_b)$ has to be taken into account.

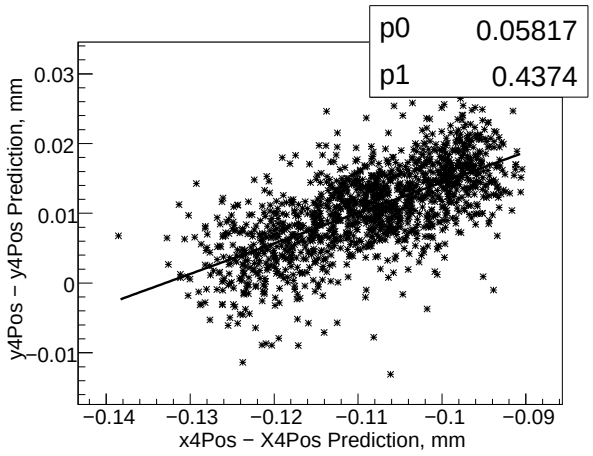

Figure 14: $y^{(4)}_{chicane}(E_b)$ versus $x^{(4)}_{chicane}(E_b)$ for an energy scan.

One possibility to include $y^{(4)}_{chicane}(E_b)$ is to perform a rotation in the (X,Y)-plane. After jitter subtraction, two new variables are defined:

$$\begin{pmatrix} (x^{(4)}_{chicane}(E_b))_{rot} \\ (y^{(4)}_{chicane}(E_b))_{rot} \end{pmatrix} = \begin{pmatrix} \cos\theta & -\sin\theta \\ \sin\theta & \cos\theta \end{pmatrix} \begin{pmatrix} x^{(4)}_{chicane}(E_b) \\ y^{(4)}_{chicane}(E_b) \end{pmatrix} . \tag{18}$$

The rotation angle $\theta = \arctan(-0.4374)$ equals to the angle of the straight line in Fig. 14. However, after normalization and comparison of $(x^{(4)}_{chicane}(E_b))_{rot}$ with x12Pos, no improvements for the beam energy resolution was noted when compared to the values calculated in the previous section. One possible reason is the less precise resolution of the measurement of (y4Pos - y^4_{jitter}) which was found to be 3.2 μm, compared to 2.3 μm (see Eq.(17) and Fig. 13). Furthermore, the value of $\theta = \arctan(-0.4374) = 23.49°$ is not alone sufficient to explain the difference between the numbers given in Eqs.(15) and (17). Indeed, the amount of rotation needed to remove this difference is

$$\begin{aligned} \frac{\sigma_{E_b}}{E_b} &= \frac{2.3\ \mu\text{m}}{5\ \text{mm} \cdot \cos\theta} = 8.5 \times 10^{-4} \\ \rightarrow \theta &= \arccos\left(\frac{2.3\ \mu\text{m}}{5\ \text{mm} \cdot 8.5 \times 10^{-4}}\right) = 57° . \end{aligned} \tag{19}$$

5 Resume

The resolution σ_{E_b}/E_b of relative beam energy measurement was measured for the 4-magnet chicane. The chicane was commissioned for the experiment

T474/491 at End Station A at the Stanford Linear Accelerator Center in 2006. The resolution σ_{E_b} is understood as to recognize variations of the beam energy bigger than σ_{E_b} from some value of the E_b, the beam energy. Some imperfect readings of the magnets, missing information on alignment and, more important, the lack of a complementary method for absolute beam energy measurement allow only to perform relative beam energy measurements, with the precisions smaller than anticipated

Since large beam jitter in the mid-chicane was observed, a method had to be developed to subtract this jitter by using informations from BPMs outside the chicane. This method is based on the assumption that the jitter at the mid-chicane can be written as a linear combination of X-, Y-positions and X-, Y-tilts from the BPMs upstream/downstream the chicane, see Eq.(10).

In order to use the BPMs downstream of the chicane it has be ensured that the upstream beam path is fully restored downstream of the chicane. Unfortunately, this condition was not achieved by the magnet chicane. Non-demagnetization and different responses of the magnets for a given current introduced an offset of beam in the BPMs downstream. This offset is correlated with the energy thereby these BPMs could not be used for the beam jitter measurements resulting to a less precise beam energy resolution.

Finally, the beam energy resolution of the 4-magnet chicane σ_{E_b}/E_b amounts to

$$\frac{\sigma_{x4Pos}^{MeV}}{E_b} = \frac{\sigma_{E_b}}{E_b} = \frac{24.3 \text{ MeV}}{28.5 \text{ GeV}} = 8.5 \times 10^{-4} \ . \tag{20}$$

This value is larger than the request of $< 10^{-4}$ for the ILC, but substantial improvements are still possible.

References

[1] M. Hildreth et al. Linear Collider - BPM-based energy spectrometer. URL http://www-project.slac.stanford.edu/ilc/testfac/ESA/projects/T-474.html, 2004.

[2] M. Slater et al. Cavity BPM system tests for the ILC energy spectrometer. *Nucl. Instrum. Meth.*, A592:201–217, 2008.

[3] Kostromin S. and Viti M. Magnetic Measurements for Magnets 10D37. Technical report, ILC-SLACESA TN-2008-1, February 2008.